CHIRP TRANSFER FUNCTION ANALYZER SIGNAL PROCESSOR

A Thesis Submitted
in Partial Fulfilment of the Requirements
for the Degree of

MASTER OF TECHNOLOGY

By

S. M. RAO

to the

DEPARTMENT OF ELECTRICAL ENGINEERING

INDIAN INSTITUTE OF TECHNOLOGY KANPUR

JULY, 1981

I.I.T. KANPUR
CENTRAL LIBRARY
Acc. No. A 66826
1 SEP 1981

EE-1981-M-RAO-CHI

CERTIFICATE

Certified that the thesis entitled "Chirp-Transfer Function Analyzer-Signal Processor", by S. Maheswara Rao is a record of the work carried out under my supervision and it has not been submitted elsewhere for a degree.

July 27, 1981

(K.R. SARMA)
Professor
Department of Electrical Engineering
Indian Institute of Technology
Kanpur-208016

POST GRADUATE OFFICE
This thesis has been approved for the award of the Degree of Master of Technology (M Tech.) in accordance with the regulations of the Indian Institute of Technology Kanpur
Dated.

ACKNOWLEDGEMENTS

I am deeply indebted to Dr. K.R. Sarma for suggesting this interesting topic and for his able guidance and encouragement throughout the course of this project.

I am grateful to Mr. Bh.A.R.B. Raju, Research Engineer, ACES, for many useful discussions I had with him. I am thankful to all other Research Engineers of ACES for their help in many ways.

I thank Mr. B.P. Choudary for the constant help rendered by him.

Many thanks are due to Mr. Rawat for the neat typing work done.

S. Maheswara Rao

ABSTRACT

Transfer function analyzer using a chirp signal as an excitation function has many advantages compared to the conventional methods of sinusoidal or pulse testing. The system architecture is discussed in this thesis. The hardware implementation of such a system has two components, (i) generation of an excitation signal and the local oscillator signals for demodulation (ii) the signal processing in the receiver to obtain the transfer function. Programmable chirp synthesizer which generates all the requisite signals is discussed in a companion thesis, "Chirp transfer function analyzer - RF programmable chirp synthesizer". This thesis covers the design and fabrication details of the hardware associated with the signal processing. A CCD chirp-Z transform chip forms the heart of the signal processing system.

CAMAC standards are followed for the hardware implementation. The transfer function of an RC low pass filter is obtained satisfactorily using the system.

TABLE OF CONTENTS

Page No.

CHAPTER I

INTRODUCTION

Time Invariant linear systems are characterized by their "system function", H(w), or impulse response, h(t). H(w) and h(t) form a Fourier transform pair [1] .

1.1 Methods of Excitation:

There are various methods to find the system function of linear systems. One method is "continuous wave excitation method", in which a pure sine wave of a fixed frequency is applied to the linear system and the output is noted after it reaches a steady state. Then the frequency of sine wave is changed by a small amount (Δf), again output is noted. The above procedure is repeated till entire frequency range of our interest is covered. In order to obtain high resolution spectrum, in continuous wave excitation, one must keep the frequency increments (Δf) very small, which consumes lot of time.

Another method is "impulse response method". In this method an impulse is applied to the linear system and Fourier transform of its time response is found to obtain the system function. But generating an impulse, with infinitesimally small width, is impracticable. So a pulse

of a finite width is used instead of an impulse. If the system function of a linear system having a bandwidth B Hz is to be found out then the pulse width should be as low as $\frac{1}{2B}$ secs. For broad band systems, i.e. systems having very large B, a pulse of very small width must be applied. Another disadvantage of pulse excitation is, it has very low average power.

The impulse response can also be measured by the correlation method [2] . The scheme for this method is shown in Fig. 1.1.

In the Figure 1.1, f(t) is the excitation to the linear system, whose impulse response is h(t), resulting in a response g(t). The excitation function, f(t), is delayed by τ and multiplied with g(t) to get p(t) which is given by

$$p(t) = g(t).f(t-\tau) = \int_{-\infty}^{\infty} h(x).f(t-x).dx.f(t-\tau)$$

Now, if we integrate p(t) over the limits $-\infty$ to $+\infty$, we get

$$\int_{-\infty}^{\infty} p(t).\,dt = \int_{-\infty}^{\infty}\int_{-\infty}^{\infty} h(x).\,f(t-x).\,f(t-\tau).\,dt.dx$$

$$= \int_{-\infty}^{\infty} h(x)\,.\,dx \left[\int_{-\infty}^{\infty} f(t-x).f(t-\tau)\;\,dt\right] \qquad (1.1)$$

The term in the paranthesis is nothing but the auto-correlation of the excitation function, f(t). If we choose

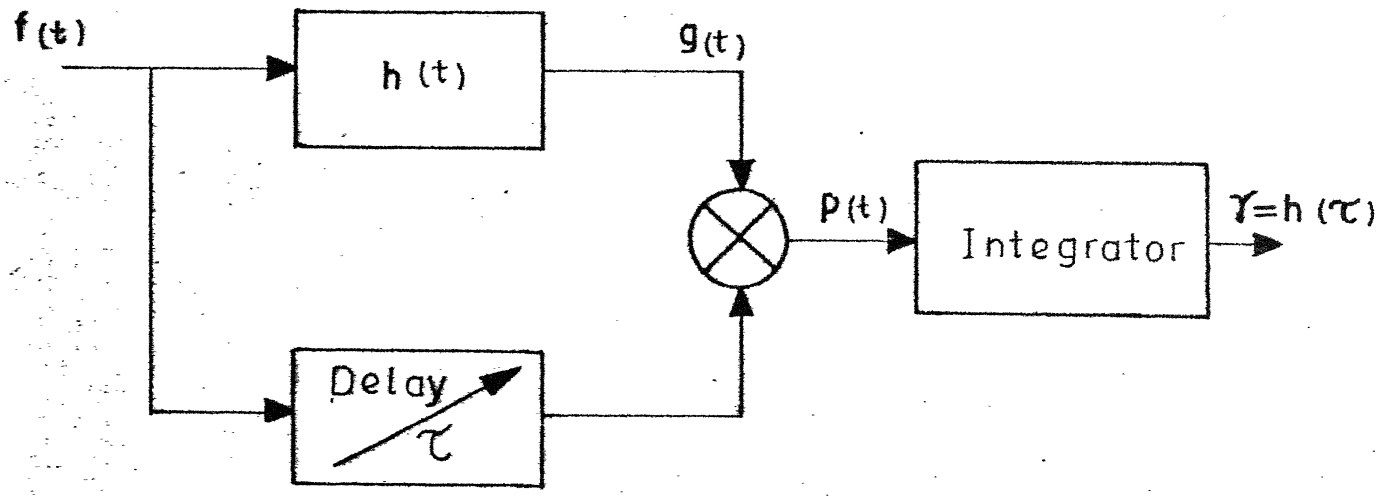

Fig.1.1 Study of excitations to the linear systems

f(t) such that its autocorrelation is an impulse function, $u_o(\tau - x)$, then integrator output, γ, is given by

$$\gamma = \int_{-\infty}^{\infty} h(x) \cdot u(\tau - x)\, dx = h(\tau).$$

By varying the delay, τ, we can get the impulse response at other points. The following two signals have the property of having autocorrelation function equal to an impulse function.

1. Psuedo Random Binary Sequence (PRBS)
2. Chirp Signal

The former one is digital in nature having only two states and the latter is analog in nature. The chirp signal also has the advantage of having larger average power when compared to pulse excitation and uniform power spectral density over its specified bandwidth. This is discussed in detail in Chapter II.

1.2 Applications:

Since a great majority of engineering systems are modelled as time invariant, there are innumerable situations requiring the knowledge of the system function and one can measure it using any of the three methods discussed above. The choice of the method is dictated by the ease of using one method over other methods. For example, nuclear spin

systems closely approximate a time-independent linear systems under non-saturating conditions [3]. Spectrum of such nuclear spin systems (NMR spectrometer) though can be obtained by using any of the above methods, the chirp technique offers some advantages in terms of instrumentation as well as accuracy.

This thesis, entitled "Chirp-transfer function analyzer - signal processor" is a companion thesis to the work done by B.P. Chowdary, towards his M.Tech. thesis entitled "Chirp-transfer function analyzer - programmable chirp synthesizer". Both the systems, put together, become a complete "Chirp-transfer function analyzer". The system has been developed for a set of specifications keeping in mind its possible use in NMR spectroscopy. That is the reason why some of the signal conditioning components, though not required for general applications, have been developed.

In Chapter II, the theory behind the operation of "chirp-transfer function analyzer" has been described. Analysis of the chirp signal is also given.

In Chapter III, power spectral density evaluation module has been described in detail and in Chapter IV,

block diagram of the proposed system, its design and circuit details of each subsystem are given. Experiments and results are given in Chapter V and conclusions and recommendations for further work are given in Chapter VI.

CHAPTER II

CHIRP TRANSFER FUNCTION ANALYZER

In this chapter the chirp transfer function analyzer is described .

Before we go in to the analysis of the chirp transfer function analyzer, a brief review of the low pass equivalent of a band pass system and the properties of the chirp signal is in order.

2.1 Low pass Equivalent of Band pass System:

A band pass signal f(t) can be written as:

$$f(t) = f_c(t) \cos w_c t - f_s(t). \sin w_c t$$

It can also be equivalently described in terms of the complex envelope as

$$f(t) = \tilde{f}(t)\, e^{jw_c t} \quad ; \text{ where } \tilde{f}(t) = f_c(t) + j\, f_s(t)$$

The low pass signals $f_c(t)$ and $f_s(t)$ are known as the inphase and quadrature components. The impulse response, h(t), of a band pass system can similarly be described in terms of its inphase and quadrature components as

$$h(t) = h_c(t) \cos w_c t - h_s(t) \sin w_c t = \tilde{h}(t)\, e^{jw_c t}$$

when the band pass signal, f(t),is fed to the band pass system with the impulse response h(t) the output g(t) is given by the convolution of f(t) with h(t) as:

$$g(t) = \int_{-\infty}^{\infty} h(x) \cdot f(t-x)\, dx$$

Substituting the equivalent low pass representations for f(t) and h(t) it can be shown that the output signal g(t) can be written as

$$g(t) = g_c(t) \cos w_c t - g_s(t) \sin w_c t = \tilde{g}(t)\, e^{jw_c t}$$

where $g_c(t) = \frac{1}{2} \mathrm{Re}\left[h(t) \otimes f(t)\right]$ and $g_s(t) = \frac{1}{2} \mathrm{Im}\left[h(t) \otimes f(t)\right]$

Thus the band pass system can be conviniently studied using the equivalent low pass systems as dipicted in Fig. 2.1

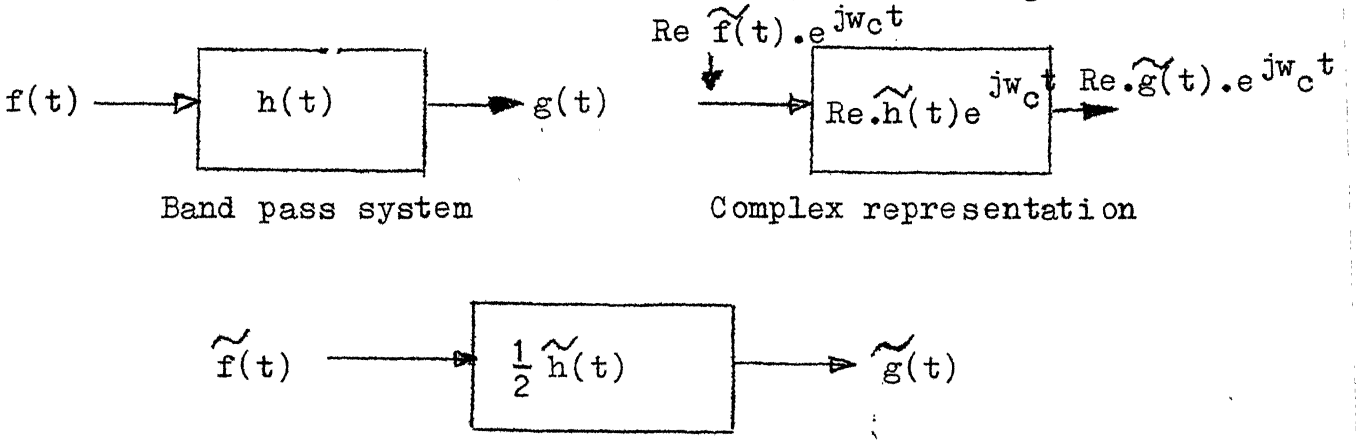

Fig. 2.1: Band pass to low pass transformation.

2.2 Analysis of Chirp Signal:

Some of the properties desired in an ideal excitation are uniform power spectral density in the specified bandwidth readily variable bandwidth and large average power. A chirp signal meets all of these requirements almost ideally [4]. First of all, it will be proved that the chirp signal has uniform power spectral density.

The chirp signal is, nothing but, a linear FM signal. So it can be represented by a mathematical expression $z(t) = e^{j\alpha t^2}$ where 2α is the chirp rate.

Case 1: Chirp signal extending from $-\infty$ to $+\infty$

Let $z(t) = e^{j\alpha t^2} \quad -\infty < t < +\infty$

$z(w)$ = Fourier transform of $z(t) = \int_{-\infty}^{\infty} e^{j(\alpha t^2 - wt)}$ (2.1)

If we put $y = \sqrt{\alpha}.t - \frac{w}{2\sqrt{\alpha}}$

we have $y^2 = \alpha t^2 + \frac{w^2}{4\alpha} - wt$ and $dt = \frac{dy}{\sqrt{\alpha}}$

hence

$$\alpha t^2 - wt = y^2 - \frac{w^2}{4\alpha} \qquad (2.2)$$

Substituting equation (2.2) in equation (2.1) we get

$$z(w) = \frac{1}{\sqrt{\alpha}} e^{-jw^2/4\alpha} \int_{-\infty}^{\infty} e^{jy^2} \cdot dy$$

$$= \frac{2}{\sqrt{\alpha}} e^{-jw^2/4\alpha} \int_{0}^{\infty} e^{jy^2} \cdot dy = \sqrt{\frac{\pi}{\alpha}} e^{j\pi/4} \cdot e^{-jw^2/4\alpha} \qquad (2.3)$$

Thus $S_z(w)$, the power spectral density of $z(w)$, defined as $S_z(w) = |z(w)|^2$, is given by

$$S_z(w) = \pi/\alpha \qquad (2.4)$$

For a chirp signal as α is a constant it gives uniform power spectral density in the specified bandwidth (in this case it is $-\infty$ to $+\infty$).

Case 2: Chirp signal is time limited ($0 < t < T$)

Let

$$z(t) = e^{j\alpha t^2} \qquad (0 < t < T)$$

$$z(w) = \int_{0}^{T} e^{j\alpha t^2} \cdot e^{-jwt} \cdot dt \qquad (2.5)$$

$$= \sqrt{\frac{\pi}{2\alpha}} e^{-jw^2/4\alpha} \left[F\left(\sqrt{2\alpha}\,T - \frac{w}{2\sqrt{\alpha}}\right) + F\left(\frac{w}{2\sqrt{\alpha}}\right) \right] \quad [5]$$

where the Fresnel integral $F(x)$ is given by

$$F(x) = \sqrt{\frac{2}{\pi}} \int_{0}^{x} e^{jy^2} \, dy$$

The asymptotic expansion for the Fresnel integral for large values of x is given by:

$$F(x) \quad \frac{1}{\sqrt{2}} e^{j\pi/4} + \frac{1}{jx\sqrt{2\pi}} e^{jx^2} + \ldots$$

Thus for large values of $\sqrt{\alpha}T - \frac{w}{2\sqrt{\alpha}}$ i.e. for $w < 2\alpha T$ the first Fresnel integral can be approximated by $\frac{1}{\sqrt{2}} e^{j\pi/4}$. Similarly for $w > 2\sqrt{\alpha}$ the second Fresnel integral can also be approximated by the first term of its asymptotic expansion. Combining the two conditions we get

$$z(w) = \sqrt{\frac{\pi}{\alpha}} e^{j\pi/4} \cdot e^{-jw^2/4\alpha} \quad w \ll 2\alpha T \text{ and } 2\sqrt{\alpha} \ll 2\alpha T \qquad (2.6)$$

The second condition in equation (2.6) can equivalently be written as $\alpha T^2 \gg 1$. It may be seen that αT is measure of the bandwidth of the signal and T is duration of the signal. Thus the quantity αT^2 is the measure of the time bandwidth product of the signal and equation (2.6) states that as long as time bandwidth product of the signal is large the frequency spectrum of the time limited chirp closely approximates the spectrum of the infinite duration chirp over a band of frequencies given by $w < 2\alpha T$.

By changing either rate of chirping (α) or time of chirping (T) we can readily change the bandwidth of the chirp

signal. Since the chirp signal has uniform power spectral density over its entire band, it does have higher average power than that of a pulse having same peak power. Therefore the chirp signal meets all the requirements for ideal excitation.

2.3 Chirp Transfer Function Analyzer:

The analysis of the chirp transfer function analyzer is carried out in terms of low pass equivalent system. The schematic of the analyzer is shown in Fig. 2.2 . Output of the chirp transfer function analyzer is given by

$$\tilde{g}(t) = \int_{-\infty}^{\infty}\int_{-\infty}^{\infty} \tilde{h}(x).e^{+j\alpha(\tau-x)^2} \cdot e^{-j\alpha\tau^2} \cdot e^{j(t-\tau)^2.\alpha} \cdot dx.d\tau$$

$$= \int_{-\infty}^{\infty}\int_{-\infty}^{\infty} \tilde{h}(x) \cdot e^{j\alpha\left[(\tau-x)^2 - \tau^2 + (t-\tau)^2\right]} \cdot dx.d\tau$$

$$= \int_{-\infty}^{\infty}\int_{-\infty}^{\infty} \tilde{h}(x) \cdot e^{j\alpha\left[\tau^2+x^2-2\tau x-\tau^2+t^2+\tau^2-2t\tau\right]} dx.d\tau$$

$$= \int_{-\infty}^{\infty} \tilde{h}(x).e^{-j2\alpha t.x} \left[\int_{-\infty}^{\infty} e^{j\alpha\left[\tau-(t+x)\right]^2} \cdot d\tau\right].dx$$

$$= \sqrt{\frac{\pi}{\alpha}} \cdot e^{j\pi/4} \int_{-\infty}^{\infty} \tilde{h}(x) \cdot e^{-j2\alpha tx} \, dx$$

$$= \sqrt{\frac{\pi}{\alpha}} \cdot e^{j\pi/4} \cdot \tilde{H}(2\alpha t)$$

So the output of the chirp transfer function analyzer directly gives the system function i.e. $\tilde{H}(2\alpha t)$.

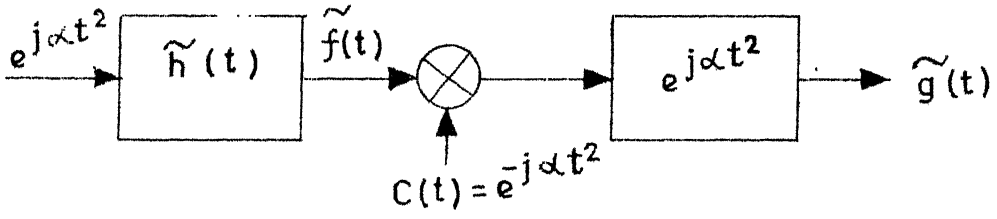

FIG.2.2 Schematic of chirp transfer function analyzer.

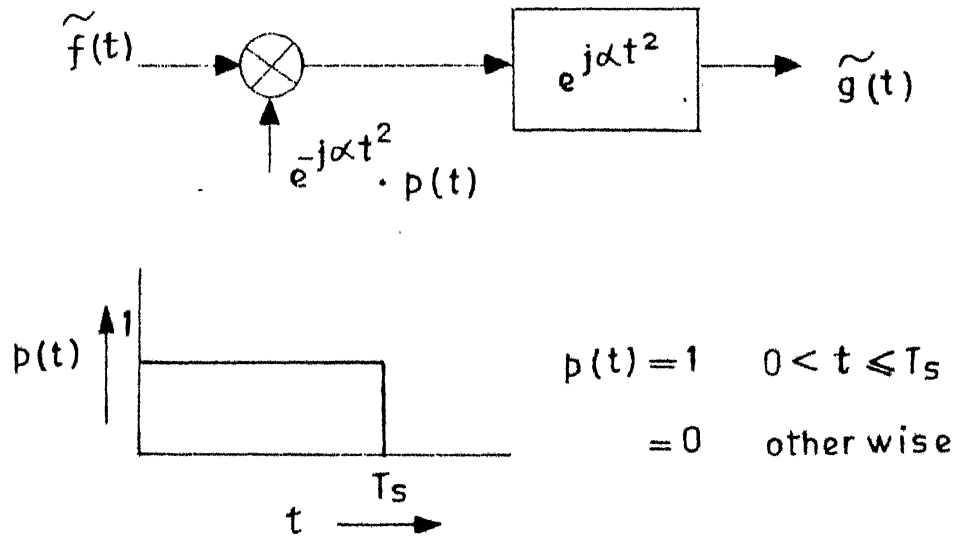

FIG.2.3 Study of the time limitedness of the chirp signal.

2.4 Limitations:

In the above derivation it has been assumed that the input chirp signal, f(t), and chirp signal, C(t), which is used for subsequent multiplication are extending from time $-\infty$ to $+\infty$. But these two chirp signals are time limited in our case. Now we study the effects of the time limitedness of these two chirp signals.

If $2\alpha T$, which is the highest frequency component of the chirp signal, is greater than the bandwidth of H(w), then the time limitedness of the input chirp signal is of no consequence. In order to study the time limitedness of the chirp signal, C(t), assume that a signal, $\tilde{f}(t)$, is applied as shown in Fig. 2.3. Time limited chirp signal can be represented as

$$e^{-j\alpha t^2} \cdot p(t) \text{ where } p(t) = 1 \quad 0 < t < T_s$$

$$= 0 \quad \text{otherwise}$$

$$\text{Then, } \tilde{g}(t) = \int_{-\infty}^{\infty} \tilde{f}(\tau) \cdot e^{-j\alpha\tau^2} \cdot p(\tau) \cdot e^{j\alpha(t-\tau)^2} \cdot d\tau$$

$$= e^{+j\alpha t^2} \int_{-\infty}^{\infty} \tilde{f}(\tau) \cdot p(\tau) \cdot e^{-j2\alpha t.\tau} \, d\tau$$

$$= e^{j\alpha t^2} \left[\tilde{F}(w) \circledast p(w) \right] \text{ with } w = 2\alpha t$$

The Fourier transform p(w) of the gate function p(t) is given by

$$p(w) = e^{-j\, wT_s/2} \quad \frac{\sin wT_s/2}{wT_s/2},$$

The "width" of p(w) is $\frac{2\pi}{T_s}$

If we approximate p(w) as impulse function then $\left|\tilde{g}(t)\right|^2 = \left|\tilde{F}(w)\right|^2$ and the condition for such approximation is $\frac{2\pi}{T_s} \ll$ Bandwidth of $\tilde{F}(w)$. So, if we satisfy the condition $\frac{2\pi}{T_s} \ll$ Bandwidth of the linear system $\ll 2\alpha T$ then the time limitedness of the chirp signal has no consequence. In practice one chooses $T_s = T$.

The above condition can be understood, more clearly, by seeing an example given below:

Bandwidth of the linear system = 10 KHz

From the first condition, we have, $\frac{1}{T_s} \ll 10\text{x}10^3$ or $T_s \gg 100\,\mu$sec

Let us take T_s as 1 millisecond.

From the second condition we have $2\pi \text{x}\ 10\text{x}10^3 \ll 2\alpha T_s$

or $\frac{2\pi \text{x} 10\text{x}10^3}{2\text{x}10^{-3}} = \pi \text{ x } 10^7$ radians/sec.

i.e. $5 \text{ x } 10^6$ Hz/sec.

So i) rate of chirping should be greater than 5×10^{6} Hz/sec.

ii) chirp width should be of the order of 1×10^{-3} secs.

2.5 Implementation:

The schematic of the implementation of the chirp transfer function analyzer for band pass systems is shown in Fig. 2.4.

The chirp signal, $\cos (w_c t + \alpha t^2)$, and the reference signals $2 \cos w_c t$, $2 \sin w_c t$ are generated by the programmable chirp synthesizer. Coherent detector processes output of the linear system, f(t), to give low pass signals $f_c(t)$, $-f_s(t)$ which are further processed by the power spectral density evaluation module (PSDE), shown with dotted lines, to give $|H(2\alpha t)|^2$.

For a low pass system, the coherent detectors are not required and the output of the linear low pass system is directly connected to the Re.input of the PSDE and Im. input is grounded.

In the next chapter the power spectral density evaluation module has been described in detail.

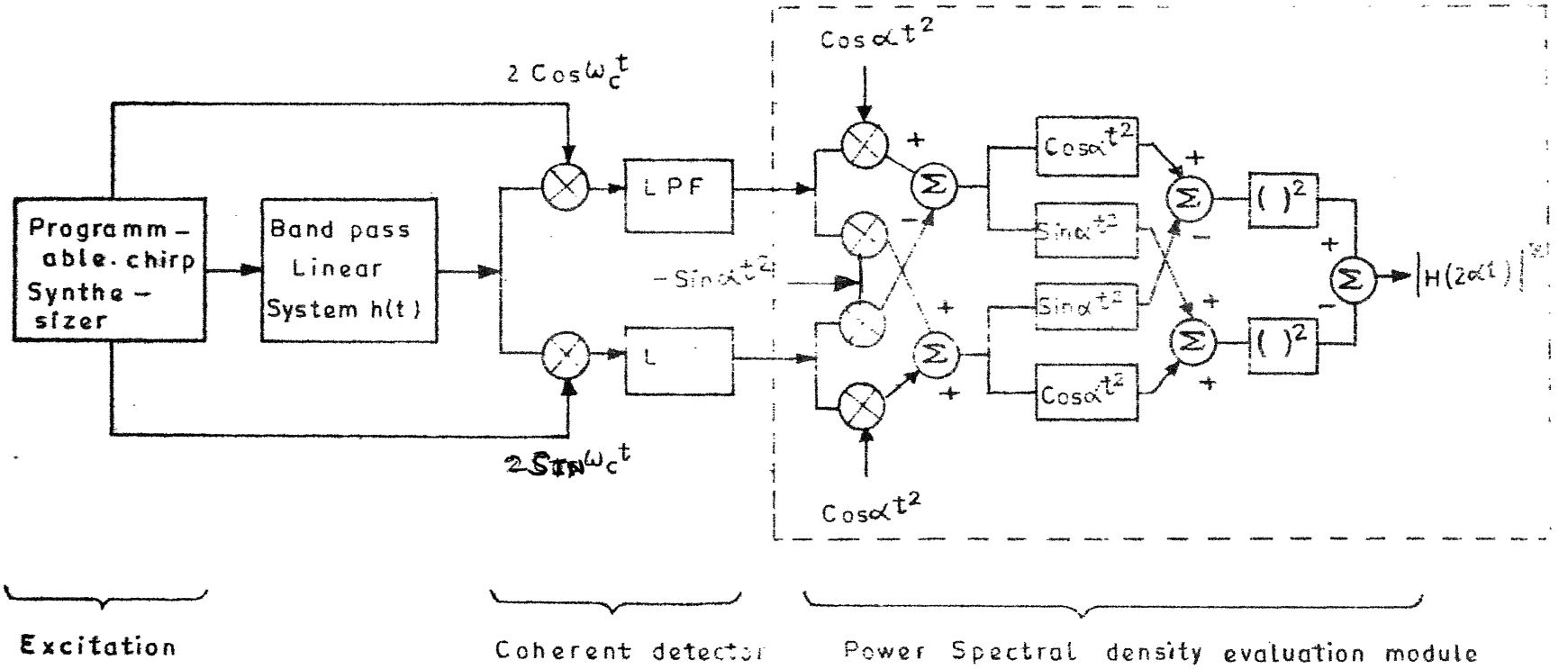

FIG.2.4 Implementation of chirp transfer function analyzer.

CHAPTER III

POWER SPECTRAL DENSITY EVALUATION MODULE

In this chapter implementation of the power-spectral density evaluation module is described in detail.

The operations involved in the PSDE module are divided in to three parts, as shown in Fig. 3.1, as (i) Premultiplication, (ii) Convolution, (iii) Hypotemuse function [6]. Implementation of these three operations is described in the following sections.

2.1 Premultiplication:

In this operation, the input signal is to be multiplied with a chirp signal, $e^{-j\alpha t^2}$. Digital techniques have been adopted to carry out this operation. The chirp signal, $e^{-j\alpha t^2}$, is approximated as $\cos \frac{\pi n^2}{N} - j \sin \frac{\pi n^2}{N}$, $1 \leq n \leq N$, where N is total number of points in the chirp signal. The chirp signal is divided into 512 samples and amplitude of each sample is represented by a 9 bit binary number. These binary numbers are stored in two Read only Memories (ROMs), one for cosine chirp and the other one for sine chirp. By addressing the locations of the ROM, one after the other, we can get back the binary information of the chirp signal. Since the input signal and resulting signal after multiplication are analog signals, we need a multiplier which

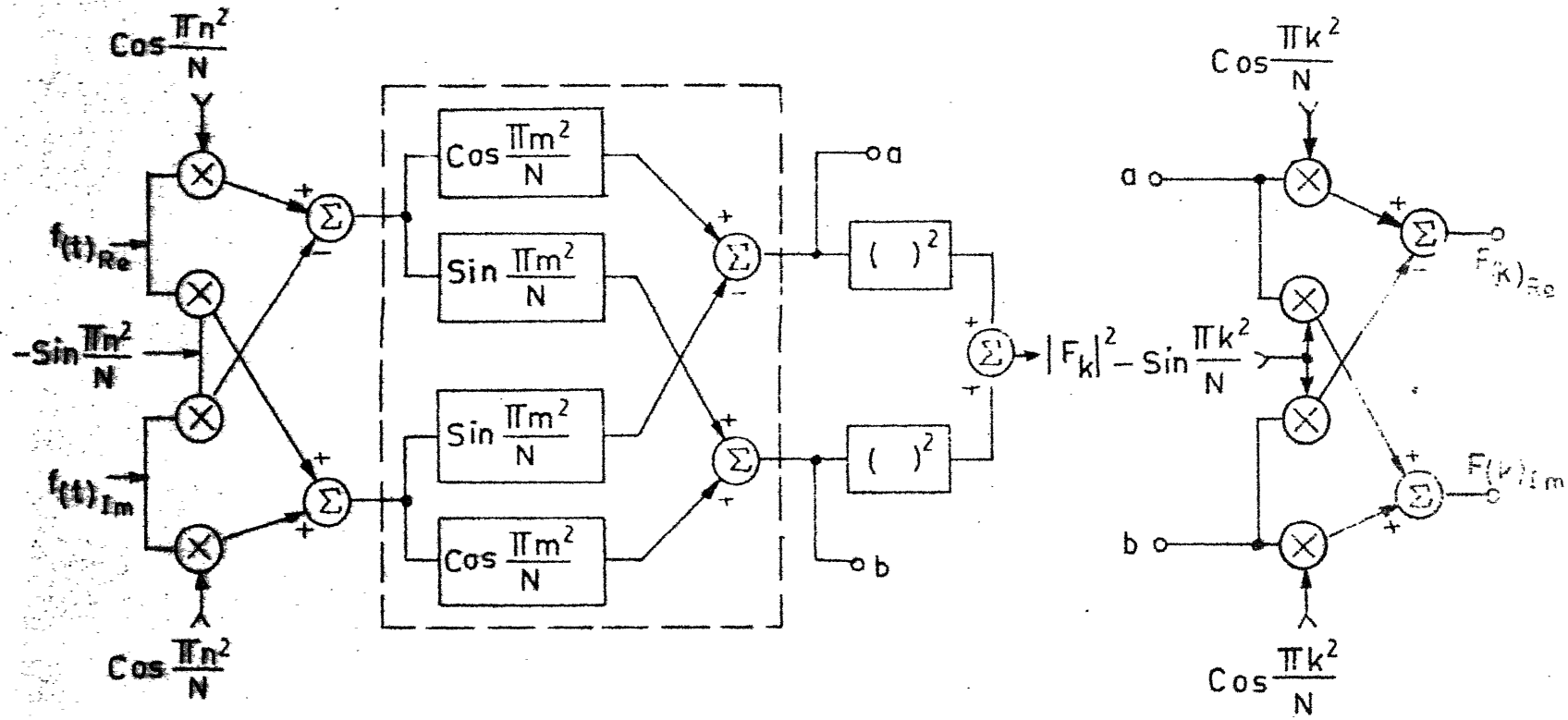

Fig. 3.1 Block Diagram for Implementation of power Spectral Density evaluation module.

accepts digital data as one of its inputs and analog input signal as its other input to give analog output. As indicated in Fig. 3.1 we need four such multipliers.

The analog input signal is buffered and converted to discrete-time samples by the input sample and hold then split in to the direct and quadrature (real and imaginary) channels. In each channel, the values are multiplied by the appropriate chirp waveform and reduced to the sampled analog product.

2.2 Convolution:

After premultiplication, we get two signals real and imaginary which are to be convolved with a complex chirp, $e^{j\alpha t^2}$. The complicated convolution is the major computing task; this task is performed by R 5601 convolution filter. It contains two separate 512-charge coupled devices which are used to implement four transversal filters using the split-electrode weighting technique [7]. The filter weighting coefficients and internal circuit connections are so that this device, with additional off chip components can implement the chirp Z transform (CZT) alogirhm [8] to calculate a 512 point DFT. The R 5601 performs the convolution of the real and imaginary input signals with a complex chirp $e^{j\pi n^2/N}$, $1 \leq n \leq 512$, $N = 512$. Some of its features are

listed below: (i) Balanced differential outputs; (ii) Dynamic range of 60 db; (iii) Sampling rates 4 KHz to 2 MHz; (iv) Filter weighting coefficient accuracy of eight bits plus sign; (v) 22-pin dual-in-line package.

2.3 Hypotenuse function:

This operation requires squaring each of the signals, real and imaginary outputs of R 5601, then combining them either directly to obtain power spectral density, or on an rms basis to obtain linear spectral density. This latter operation is approximated by the absolute value amplifiers and the hypotenuse amplifiers. That is, $\sqrt{a^2+b^2}$ is approximated by adding the magnitude of the larges signal to a fraction, K, of the magnitude of the smaller signal. $\sqrt{a^2+b^2} \approx |\text{larger}| + K\,|\text{smaller}|$, where the factor K is in the range 0.3 to 0.5. This approximation is in error by less than 2% when the ratio of the two signals is greater than 2:1, but because of the error, the amplitude of spectral lines have a "jitter" of approximately 10% when the input signal is not synchronous with the sample frequency. The rms amplitude is preferable to the power spectral density because of the lesser dynamic range required, for input having 60 db dynamic range, an output (voltage) proportional to power would have 120 db dynamic range.

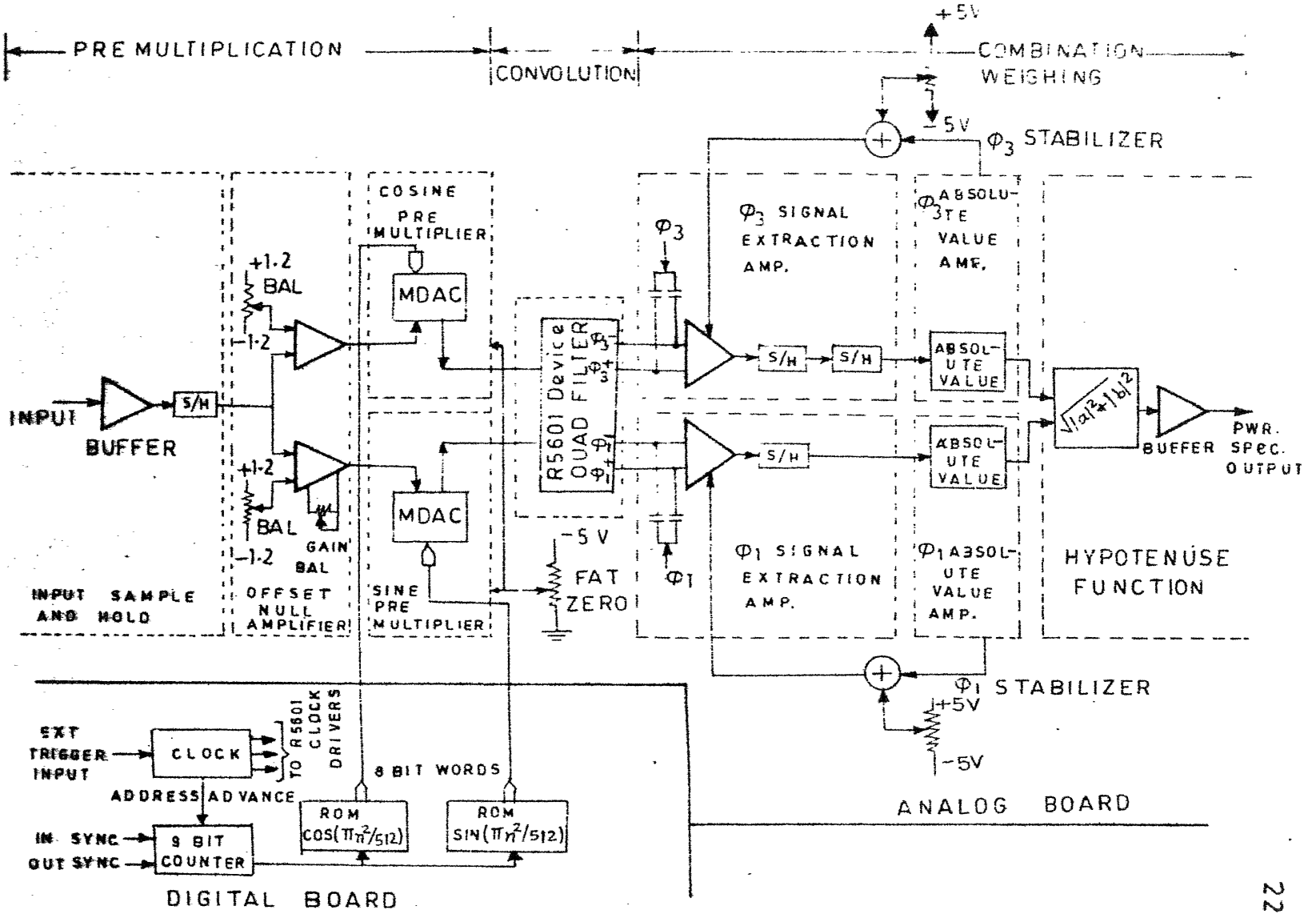

Fig. 3.2 Block Schematic of Chirp-z transform Spectrum Analyzer.

Implementation of all the above three operations are clearly indicated in Fig. 3.2.

2.4 External Triggering:

The analysis band in the normal situation extends from zero to the Nyquist frequency (one-half the sample frequency). The resolution bandwidth is approximately $\frac{1}{5}\%$ of the sample frequency ($\frac{1}{512}$). When internally triggered it is set to a sample frequency of 100 KHz and resolution bandwidth 200 Hz. Provision is made for an external system trigger which will permit operation at lower sample rates if desired. The trigger pulses (0.5 μ sec, positive going) must be at the desired sample rate. The nine-bit address to address ROMs is generated in a counter advanced once per input trigger pulse. All the timing is controlled by a self-contained clock to control the various sample and hold circuits and clock phase elements before advancing to the next sample and next ROM address.

CHAPTER IV

DESIGN AND CIRCUIT DETAILS

In this chapter the complete block diagram of the "chirp transfer function analyzer - signal processor" is given. Design details of each module and circuit diagrams are also given.

4.1 Block Diagram Description:

The complete block diagram of the chirp transfer function analyzer-signal processor is given in Fig. 4.1

In the above block diagram the amplifier-attenuation combinations caters for the wide dynamic range of the input signals and provides a fixed signal level to the coherent detector. The coherent detector is required only in the case of band pass signal inputs. For the low pass signal inputs, the coherent detector is bypassed. The local oscillator signals to the coherent detector are obtained from the programmable chirp synthesizer. The power density spectral evaluation (PSDE) module, described in detail in Chapter III, processes the inphase and quadrature inputs and gives the system transfer function at the output. It may be recalled that in case of low pass signals, the PSDE module has only one input. The sweep generator provides

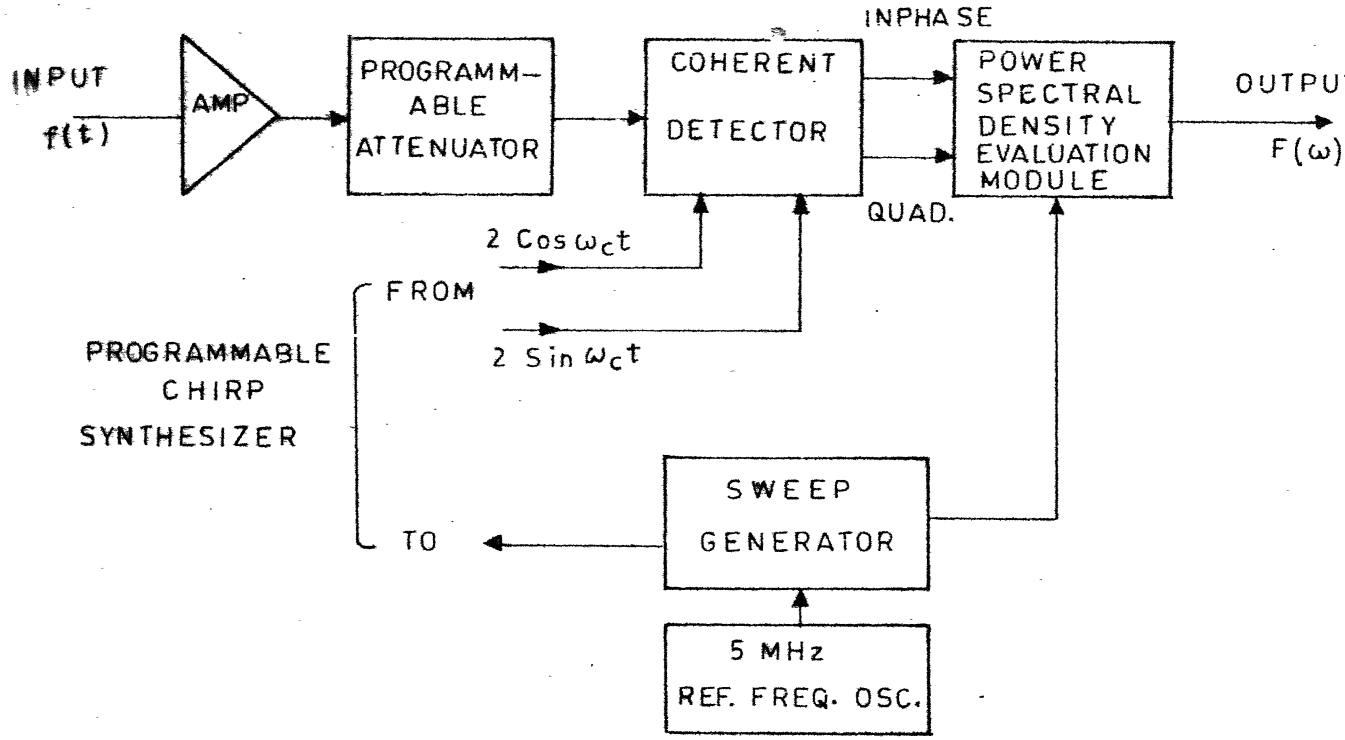

Fig.4.1 BLOCK DIAGRAM OF CHIRP TRANSFER FUNCTION ANALYZER SIGNAL PROCESSOR

timing signals to PSDE module and the excitation unit, programmable chirp synthesizer. As the sweep generator and the programmable chirp synthesizer have a common 5 MHz reference from a crystal oscillator, the sweep generator keeps the whole system in perfect synchronism.

In the next few sections the specifications and design details of each subsystem have been described.

4.2 Specifications:

In this section specifications of each module are given. The indicators that are given on the front panel of each module are given in paranthesis.

(A) Sweep Generator:

(i) Inputs : (a) 5 MHz reference frequency from a crystal oscillator (5 MHz REF IN)

(b) Positive going TTL trigger pulses (TRIGGER IN)

(ii) Outputs: (a) Sampling pulses output (SAMPLING OUT)

(b) Ramp out (RAMP OUT)

(iii) Ranges : (a) Sampling rate: 1 sec to 10 secs in 5,2,1 sequence

(b) Ramp: width: is variable from 0.512 ms in 5,2,1 sequence

Amplitude: is adjustable from 500 mV to 10 volts.

Resolution: 9 bit resolution.

(iv) Front panel controls: (a) Toggle switch for local/ remote selection (REMOTE/ LOCAL)

(b) Toggle switch for mode selection(TRIGGERED MODE/ FREE RUN MODE)

(c) Thumb wheel switch for range selection(SWEEP RANGE)

(d) Lever switch for 5,2,1 sequence selection (x1, x2, x5)

Note: The above switches are common for sampling out and Ramp out.

(v) Packaging : In conformance with the international CAMAC Standard for nuclear modules [9].

(vi) Power supplies : (a) +5V supply (for digital purposes) has been derived from +6V CAMAC bus line.

(b) +5V supply (for analog purposes) has been derived from +12V CAMAC bus line.

(c) -5V (for analog purposes) has been derived from -12V CAMAC bus line.

(d) +12V & -12V supplies to drive op.amps. have been taken directly from the +12V & -12V CAMAC bus lines respectively.

(B) Programmable Attenuator:

(i) Input : Signal that is to be attenuated (INPUT)

(ii) Output : Attenuated signal (OUTPUT)

(iii) Ranges : (a) input signal frequency: DC to 500 MHz

(b) Attenuation : 0 to 63 db in steps of 1 db

(c) input signal level : +20 dbm max.

(iv) Front panel controls: (a) Thumbwheel switches for attenuation setting (ATTENUATION DB)

(b) Toggle switch for local/remote selection (REMOTE/LOCAL)

(v) Packaging : In conformance with the CAMAC Standard for nuclear instruments

(vi) Power supplies : (a) +5V supply (digital purposes) has been derived from +6V CAMAC bus line.

(b) +6V, -6V supplies have been taken directly from +6V, -6V CAMAC bus lines respectively.

(C) Pre-amplifier and Coherent Detector :

(i) Inputs: (a) RF signal input to the preamplifier (RF IN1)

(b) RF input to the coherent detector (RF IN2)

(c) Inphase LO input to the coherent detector (REF IN)

(d) Quadrature LO input to the coherent detector (QUAD IN)

(ii) Outputs : (a) Output of the preamplifier (RF OUT 1)

(b) Inphase component of the coherent detector output (REAL OUT)

(c) Quadrature component of the coherent detector output (IMAG OUT)

(iii) Ranges : (a) Input frequencies: 1) Input frequency to the preamplifiers: 5 MHz to 250 MHz

2) Input frequency to the coherent detector: 5 MHz to 500 MHz

3) Inphase/quadrature input to the coherent detector: 5 MHz to 500 MHz.

(b) Input signal levels: 1) Input to the preamplifier: 550 V (max)

2) Input to the coherent detector: +2.5 dbm (Typical)

3) Inphase/quadrature inputs to the coherent detector: 0 dbm (typical)

(c) Sensitivity of the preamplifier : -86 dbm @ 290°K

(iv) Power supplies : (a) +15 volts supply has been derived from +24 volts CAMAC bus line

(b)+12V & -12V supplies have been directly taken from +12V & -12V. CAMAC bus lines respectively.

(v) Packaging : In conformance with the CAMAC Standards for nuclear instruments.

4.3 Design Details:

In this section circuit schematics of each module have been described. Each subsystem has been designed in accordance with the "CAMAC Standards". Data can be entered in to these subsystems either through the CAMAC dataway or through Front panel switches. So in each module an interfacing circuit is used, which has been described below and shown in Fig. 4.2.

Programmable Peripheral Interface (PPI) INTEL (8255) acts as an interface between Read lines, write lines of CAMAC dataway and Data port B of the multiplexer. Control and decoding logic decodes the instruction, given through the CAMAC Dataway, and controls the PPI. Select switch REMOTE/ LOCAL determines whether the data to the module is coming from Data port A or Data port B. When this switch is in "REMOTE" position, PPI will be in operation and the data port

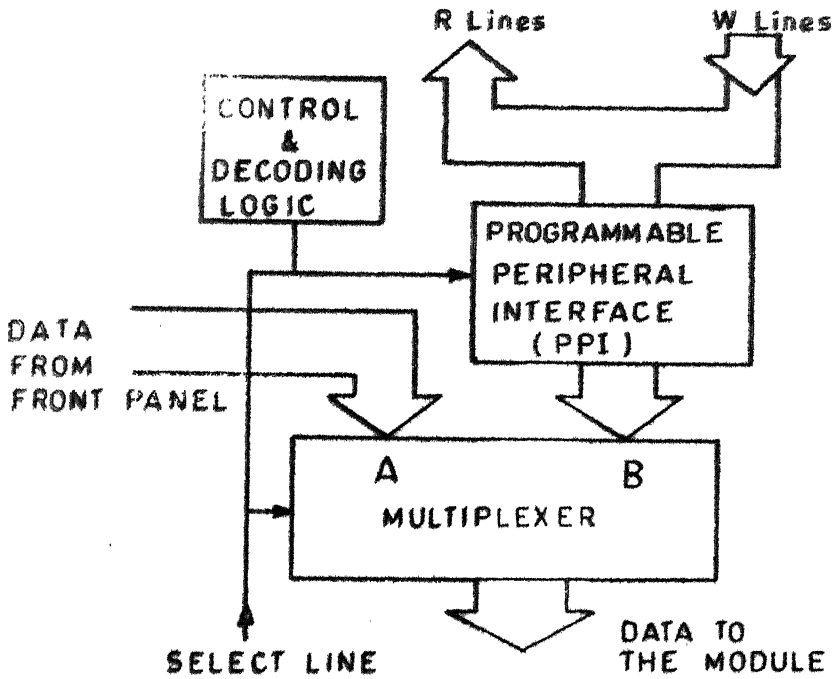

Fig.4.2 SCHEMATIC OF THE INTERFACING CIRCUIT

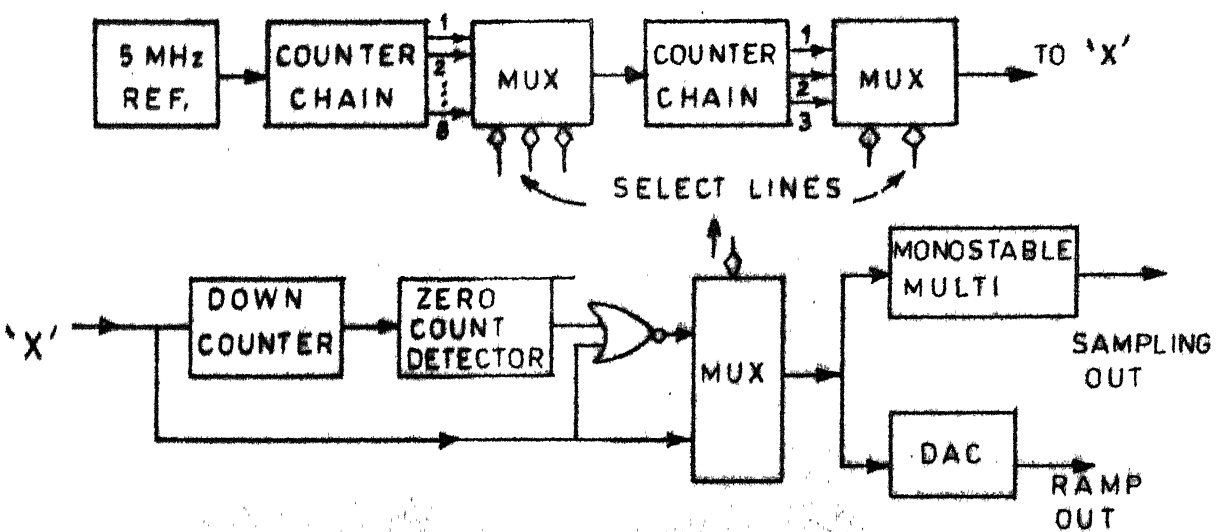

Fig. 4.3 BLOCK SCHEMATIC OF THE SWEEP GENERATOR

I.I.T. KANPUR
CENTRAL LIBRARY
Acc. No. A 66826

B will be connected to the output. When it is in LOCAL position the PPI is temporarily cut-off and data port A is connected to the output.

4.3.1 Sweep Generator:

Block diagram of the sweep generator is given in Fig. 4.3. 5 MHz reference frequency from crystal oscillator is divided by a chain of eight decade counters (7490) to get signals of various time periods. Among these eight signals any one signal can be selected by three select lines of MUX 1 (74 151). The selected signal frequency is further divided by another decade counter to get ÷1, ÷2, ÷5, frequencies. Again one of these three signals can be selected by 2 select lines of MUX 2 (74153). Output of MUX2 goes to one of the inputs of MUX3 (74153) to give free running mode signal. Output of the MUX2 also goes to a cascaded chain of decade counters (7419), which are connected in down count mode and whose output goes to the other end of MUX3 through a NAND gate to give triggered mode signal. Initially the down counter is loaded with the number 512. For each input pulse the down counter counts down starting from 512. As soon as this count becomes zero, zero count detector output will go to a '1' level. So the NAND gate output stays at a low level irrespective of the other input. To start the operation again, the down counter is to be loaded with the

number 512 and the output of the zero count detector is to be reset to low level. Output of the MUX3 is given to a monostable multi (74121) to get fixed duration (0.5 sec.) +ve going pulses which are used to drive the power spectral density evaluation module. The same signal, i.e. MUX3 output, is also given to a DAC (TDC 1016J) to get the ramp output which is used to drive the programmable chirp synthesizer. Complete circuit diagram is given in Fig. A.

4.3.2 Programmable Attenuator:

It is a signal conditioning unit in which attenuation can be programmed from 0 db to 63 db. Block diagram of programmable attenuator is shown in Fig. 4.4.

This subsystem is nothing but an interfacing system to the programmable attenuator (100-12-SMA;DIACO). This interfacing system consists of Buffers (7406) to drive the transistor (BC 149) which is turn drive the input circuits of the programmable attenuator.Data from the front panel, which is in BCD frform, is converted into binary equivalent (using 74184) to make the circuitry compatible with the other data port, namely, CAMAC data way. Complete circuit diagram of the programmable attenuator is given in Fig. B.

4.3.3 Pre-amplifier and Coherent Detector:

Block diagram of this module is given in Fig. 4.5.

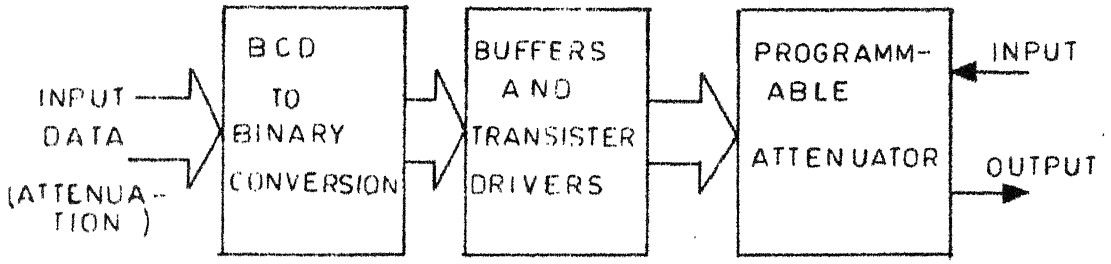

FIG.4.4 Block diagram of the programmable attenuator.

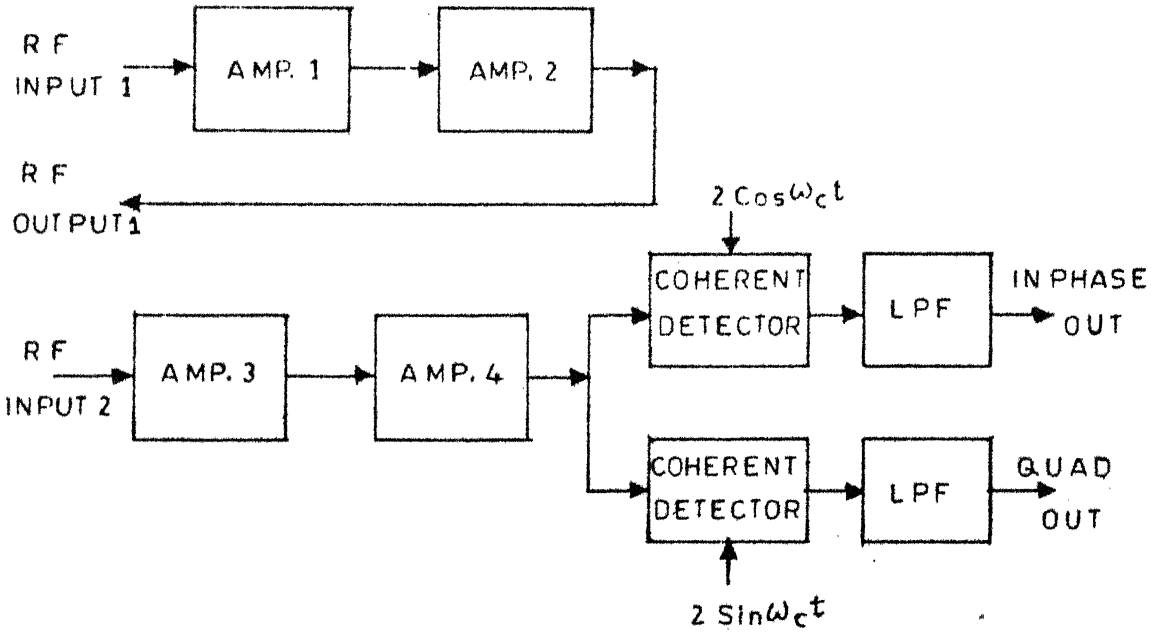

FIG.4.5 Block diagram of pre amplifier and coherent detector module.

In this module the four identical amplifiers are so arranged that using the programmable attenuator, described above, the signal level at the coherent detector can be kept to lie with in its dynamic range. Amplifier I and amplifier II are separated from other amplifiers and these can be used as preamplifiers, if required. WJA74-1's are used for these amplifiers, whose specifications are given below [10].

Frequency Range	:	5 MHz to 250 MHz
Small signal gain	:	30.0 db (Typical)
Gain flatness	:	$\pm$ 1 db
Noise figure	:	5.0 (Typical)
Dynamic range of all amplifiers	:	-85 db

MD-108 double balanced mixers are used for coherent detector. Low pass filters are designed for Fourth order Butterworth response and cut-off frequency f_c at 10 KHz, using standard realization techniques [11]. Complete circuit diagram with component values is given in Fig. C.

CHAPTER V

EXPERIMENTS AND RESULTS

In this chapter experiments that are conducted and their results are discussed.

5.1 Sine Wave Testing:

A pure sine wave of 200 mV (peak to peak) is given to the PSDE module and its output is observed on an oscilloscope. Its spectral line, which moves in the horizontal direction with the input frequency and whose amplitude changes with input signal amplitude is observed. The input sine wave and its spectrum are shown in Figures 5.1(a) and 5.1(b) respectively. The resolution of frequency band is verified by applying two sine waves simultaneously. When the internal sampling rate of 100 KHz is used, the two signals can be resolved only when their frequency difference is 200 Hz or more which is equal to $\frac{1}{T}$ with T=512x10 μ sec.

5.2 Square Wave Testing:

A square wave of 10 KHz, 200 mV (peak to peak) is applied to the PSDE module and its output, the spectrum of the square wave is observed on the oscilloscope. Variations of the spectrum with input frequency, amplitude

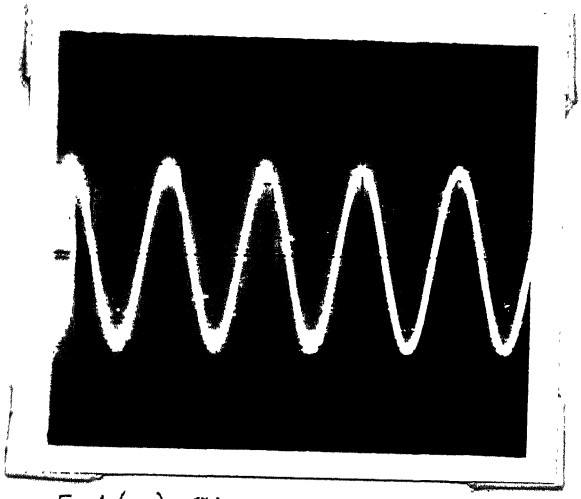

5.1(a) Sine wave

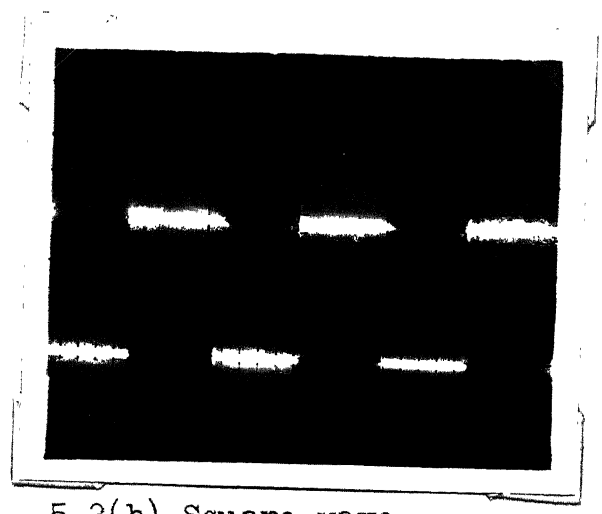

5.2(b) Square wave

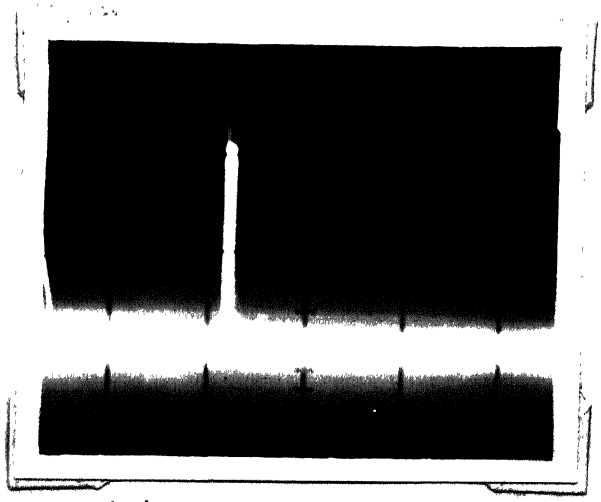

5.1(b) Spectrum of sine wave

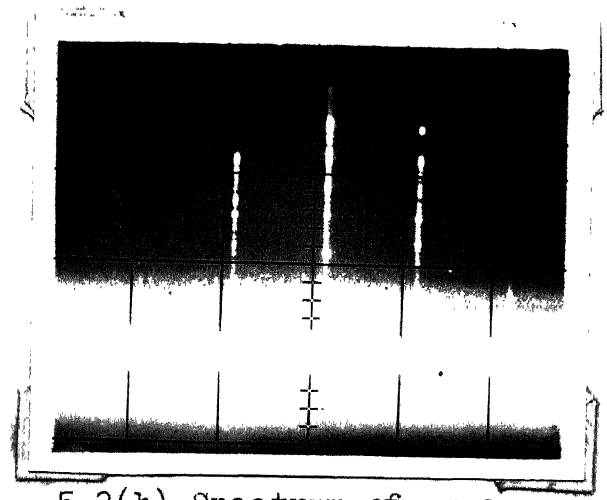

5.2(b) Spectrum of square wave

and duty cycle are observed and found that they are varying correctly. The input square wave and its spectrum are shown in Figures 5.2(a) and 5.2(b) respectively.

5.3 PSDE Module as an Optimum Receiver:

The structure of the PSDE module is identical to the optimum receiver for estimating the frequency of a sinusoid immersed in noise. A detailed analysis of the optimum receiver is given in [12] . Experimental setup, to estimate the frequency of a sinusoid immersed in noise, using the PSDE module, is shown in Fig. 5.3. A pure sinusoidal signal, generated by the test oscillator, is summed up with the output of the random noise generator, and given to the PSDE module. Now by varying the noise level output of the PSDE module is observed in the oscilloscope.

It is observed that the output of the PSDE module is nothing but the spectrum of the sinusoid, upto certain noise level. If the noise level is increased, then amplitude of the signal spectrum falls slowly and reaches a point where we can not detect the signal any more. Readings are taken to find the signal to noise ratio at this point and they are tabulated below.

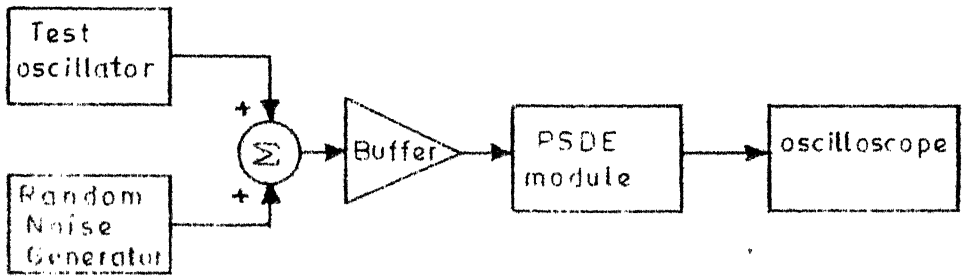

FIG. 5.3 Experimental set up to verify that the PSDE module acts as an optimum receiver.

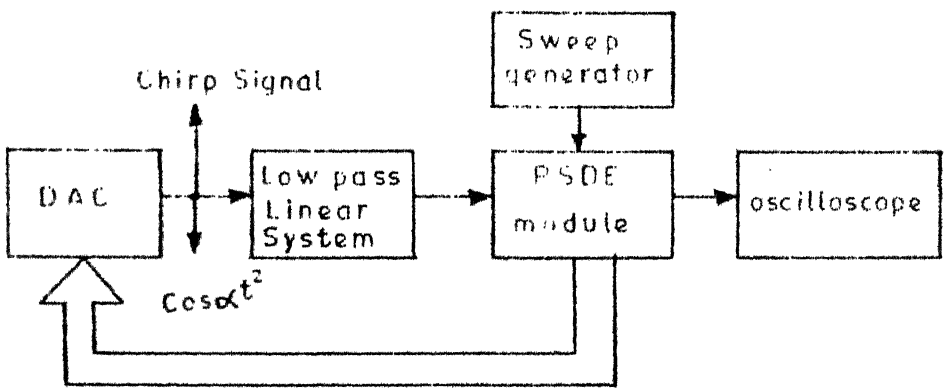

FIG. 5.4 Experimental set up for low pass system testing.

Sl. No.	Noise frequency	Amplitude of the signal (A)	Amplitude of the noise(σ)	S/N= $\frac{A^2/2}{\sigma^2}$	S/N in db
1	5 MHz	0.34 volts	1.666 volts	1/50	-17 db
2	500 KHz	1.4 volts	7.500 volts	1/50	-17 db

In the above table, σ is calculated by measuring peak to peak voltage of the noise signal and dividing this value by a factor of 6. The sine wave immersed in noise and its spectrum are shown in Figure 5.5(a) and 5.5(b).

5.4 Low Pass System Testing:

Experimental set up for testing system function of low pass systems is shown in Fig. 5.4.

Chirp signal, $\cos \alpha t^2$, which is applied to the linear system is derived from the PSDE module. A simple RC low pass filter is used as the low pass system. Its output is given to the PSDE module, which is triggered externally by the sweep generator. Output of the PSDE module is seen on the oscilloscope. The pattern on the oscilloscope closely resembled the system function of the low pass filter.

By changing the cut-off frequency of the low pass filter, the corresponding changes in the output of PSDE module are observed and found that the system can be conviniently used for finding system function of any time invariant linear system. The input chirp signal, output of the low pass filter and output of the PSDE module are shown in Figures 5.6(a), 5.6(b) and 5.6(c) respectively.

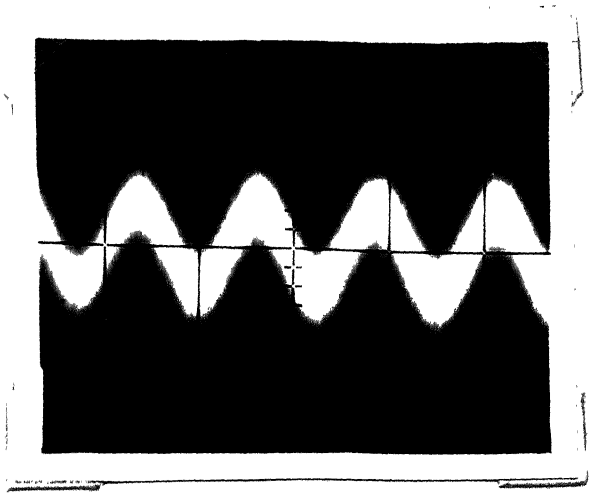

Fig. 5.5(a) Sine wave
immersed in noise

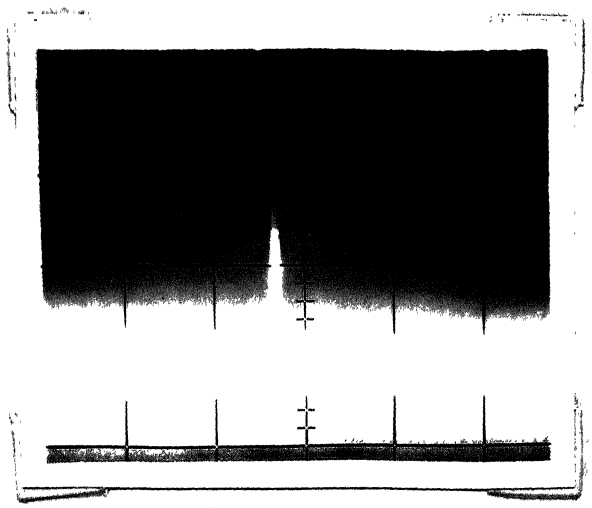

Fig. 5.5(b) Spectrum of sine
wave immersed in noise

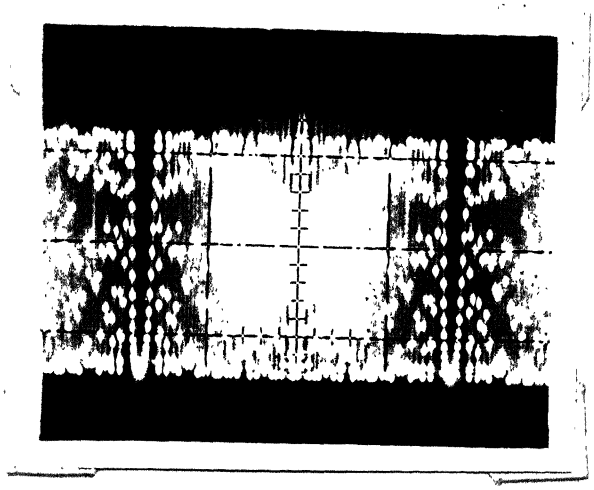

Fig. 5.6(a) (i) Input chirp signal

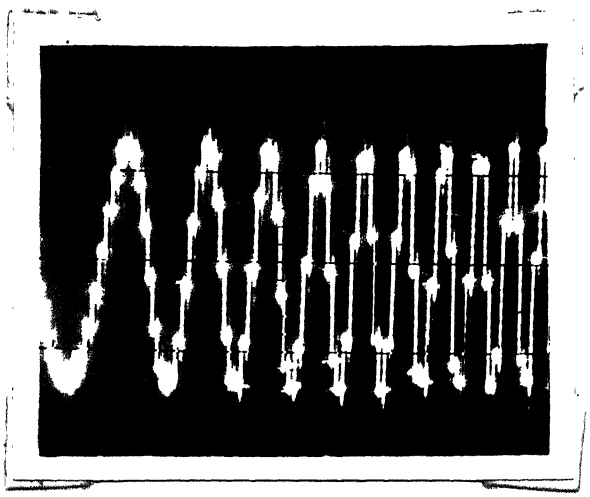

(ii) Input chirp enlarged version.

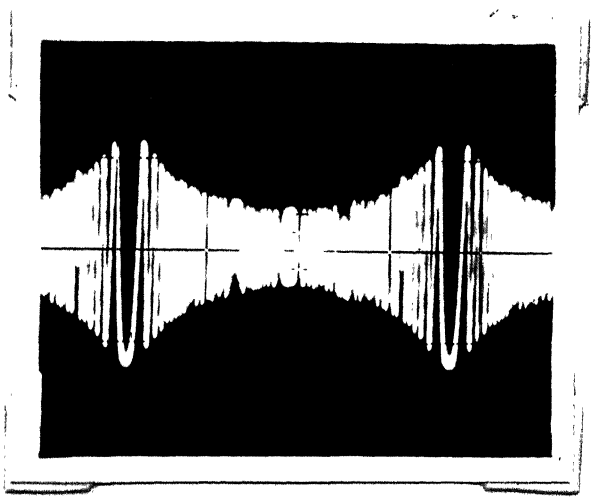

Fig. 5.6(b) Output of the low pass filter.

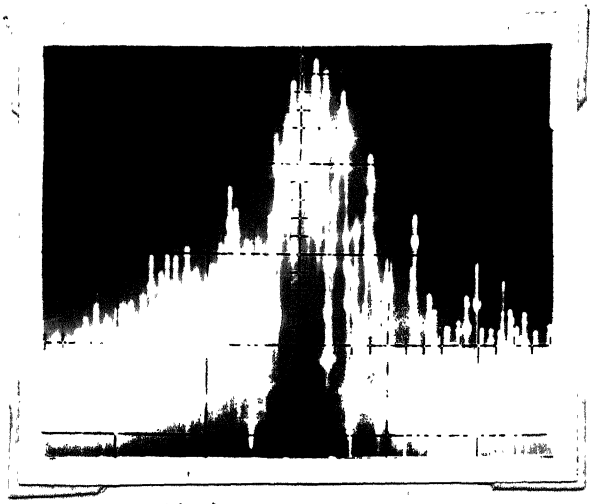

Fig. 5.6(c) System function of the low pass filter

CHAPTER VI

CONCLUSIONS AND SUGGESTIONS

Chirp transfer function analyzer which finds the system function of a band pass linear system, using the chirp signal as excitation, is described. CAMAC standards are followed for its hardware implementation. Usually data to the modules is entered through the CAMAC data bus using a computer, but, where computer is not available the data can also be entered through front panel controls. Some experiments have been conducted on the PSDE module and their results are described. The chirp transfer function analyzer is tested for a low pass linear system.

The PSDE module that is used here suffers from poor frequency resolution. Frequency resolution of the PSDE module can be improved by enhancing the number of points in the spectrum. Presently, it has 512 points and by increasing this number to 1024 or more the frequency resolution can be improved by a factor of 2 or more. In the existing PSDE module we can not increase the number of points readily, because the chip R5601 has a limited capacity of 512 points.

For the band pass system testing, PSDE module with two input channels is required. As the existing PSDE

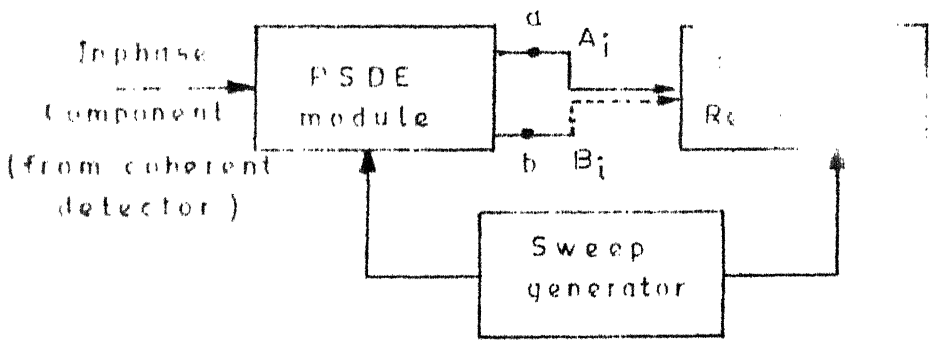

(a) With Inphase component

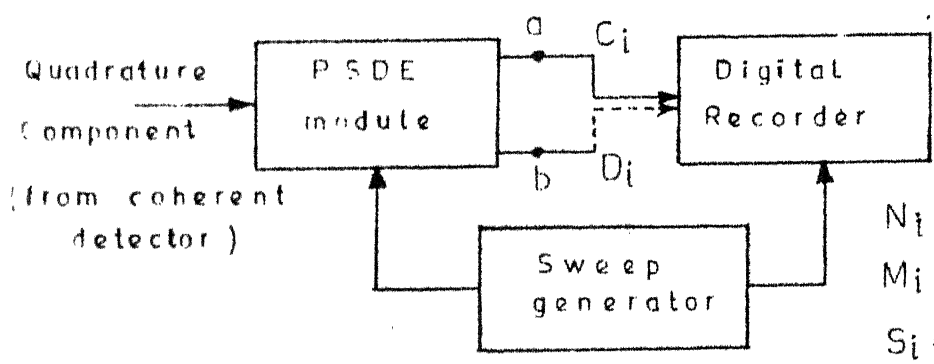

$N_i = A_i - D_i$

$M_i = B_i + C_i$

$S_i = \sqrt{N_i^2 + M_i^2}$

$i = 1, 2, 3 \ldots, 512$

(b) With Quadrature Component

FIG.6.1 Procedure for bandpass linear system testing.

module has only the Re. input channel the band pass system testing could not be done. The 'Im' input channel can be developed using one buffer, one sample and hold circuit and two multiplying DACs. However even with the existing PSDE module band pass linear systems can be tested by the procedure, shown in Fig. 6.1, which is self explanatory.

In the above figure terminals a and b are same as terminals a and b in Fig. 3.1. First, all A_is are recorded in any digital recorder and then B_is are recorded. System function can then be obtained by computing all S_is, in accordance with the relationships shown in Fig. 6.1.

Chirp transfer function analyzer is developed keeping in mind its possible use in NMR spectrometer. This system need be tested, for its feasibility as an add on to a CW NMR spectrometer.

REFERENCES

1 PAPOULIS, A. : "Signal Analysis"
McGraw-Hill Book Company; 1977
pp. 15-21.

2 LANING & BATTIN: "Random processes in automatic control";
McGraw-Hill Book Company, Inc. NY, 1956.

3 RAJ K. GUPTA et al: "Rapid Scan Fourier Transform NMR Spectroscopy";
vol. 13; Journal of Magnetic Resonance, 1974
pp. 275-290.

4 JOSEPH DADOK et al: "Correlation NMR Spectroscopy"
Journal of Magnetic Resonance; vol.13, 1974,
pp. 243-248.

5 PAPOULIS, A.: "Systems and transforms with applications in optics"
McGraw-Hill Book Company, 1968
pp. 67-74.

6 RETICON CORP.: "RC 5601 Power Spectral density board, operating instructions"
Reticon Corporation, 1978.

7 BRODERSON, R.W. et al: "A 500-stage CCD transversal filter for spectral analysis"
IEEE Journal of solid-state circuits,
SC-11, No. 1, Feb, 1976;
pp. 75-84.

8 RABINER, L.R. et al: "The chirp Z-transform algorithm"
vol. AU-17, June 1969,
pp. 86-92.

9 IEEE, Inc. : "CAMAC instrumentation and interface standards"
IEEE, Inc., 1976
pp. 7-51

10 WATKINS-JOHNSON COMPANY : "RF SIGNAL PROCESSING COMPONENTS" Data Manual, Watkins Johnson Company,197 pp. 90-91

11 MILLMAN & HALKIAS: "Integrated Electronics: Analog and digital circuits & systems" McGraw-Hill KOGAKUSHA LTD., 1972 pp. 548-553.

12 VITERBI, A.J.: "Principles of coherent communication" McGraw-Hill Book Company; 1966 pp. 283-286.